International Journal of Development Mathematics Vol 2 Issue 1 Page No. 186 - 199

INTERNATIONAL JOURNAL OF DEVELOPMENT MATHEMATICS

ISSN: 3026-8656 (Print) | 3026-8699 (Online)

journal homepage: https://ijdm.org.ng/index.php/Journals

Effect of Relaxation Time from Improved Bloch NMR Fluid Flow Equation on Area under NMR Spectrum of Blood Spinning Protons using Fourier Transform Method

Rasheed A. Lateef[a*], Usman Adam[a] and Timtere Pascal[a]

[a]Department of Physics, Faculty of Physical Sciences, Modibbo Adama University, Yola, Adamawa State, Nigeria

ARTICLE INFO

Article history:
Received 10 December 2024
Received in revised form 14 March 2025
Accepted 21 March 2025

Keywords:
Fourier transform, area under NMR spectrum, Improved Bloch NMR fluid flow equation, Blood vessels.

MSC 2020 Subject classification:
42B10, 44A10, 47A10, 34A30, 35M20

ABSTRACT

This study aims to develop a new NMR spectrum governing equation. It also investigates theoretically the effect of transverse relaxation times of arterial, venous, and capillary blood samples on the area under the spectrum of blood proton spins. Laplace transform method was used to build the NMR signal equation, which is the solution of the improved Bloch NMR time-dependent fluid flow equation. Furthermore, Fourier transform signal processing technique was used to convert the NMR signal to the NMR spectrum. MATLAB and Origin Pro software tools were utilized as primary tools for d*ata generation and simulation purposes. The results for arterial, venous, and capillary blood samples illustrated that the area under the spectrum (As) varied as a function of changes in the transverse relaxation time, T2. Firstly, for arterial blood, when T2 = 228 ms, 245 ms, 262 ms, and 279 ms, the computed values of As = 0.02155 Aradm-1s-1, 0.02150 Aradm-1s-1, 0.02141 Aradm-1s-1, and 0.02097 Aradm-1s-1, respectively. Additionally, for venous blood, when T2 = 158 ms, 173 ms, 188 ms, and 203 ms, the computed values of As = 0.02416 Aradm-1s-1, 0.02334 Aradm-1s-1, 0.02270 Aradm-1s-1, and 0.02259 Aradm-1s-1 respectively. In conclusion, for capillary blood, when T2 = 10 ms, 73 ms, 136 ms, and 199 ms, the computed values of As = 0.00127 Aradm-1s-1, 0.01365 Aradm-1s-1, 0.02697 Aradm-1s-1, and 0.02530 Aradm-1s-1 respectively. These results mean that as blood circulates through the human blood vessels, the number of spinning protons changes due to varying transverse relaxation times of arterial, venous, and capillary blood. The results of the simulation may be used by spectroscopists to verify experimental results in order to determine the number of nuclei, resonant frequency, and chemical shift of nuclei in a sample.

1. Introduction

Fourier transform (FT) is a mathematical transformation used to convert time-domain signal, also known as free induction decay (FID) signal, to frequency domain signal, which is also known as NMR spectrum (Farrar, 1978; Hosur and Kakita, 2022; Hulse, 2023). This can be used in a variety of fields, including data analysis, image processing, and signal processing (Chittora and Babel, 2018; Sifuzzaman *et al*., 2009). FT is named after a French mathematician called Jean-Baptist Joseph Fourier, who was the first to develop the theory (Tasiu and Usman, 2024). In addition, FT can be applied in nuclear magnetic resonance imaging (MRI), where it is used to convert MRI data into images of the inside of the body (Bottomley, 1983; Katti *et al*., 2011). FT has also been applied in other fields of chemistry, such as infrared (IR) and mass spectrometry (MS). FT is used in MS to transform the raw mass spectrum into a signal with high resolution and sensitivity. FT is used in IR spectroscopy to convert the raw data into a spectrum that shows the chemical bonds and functional groups that are present in a molecule (Dutta, 2017; Hsu, 1997; Tsybin *et al.*, 2019).

Nuclear Magnetic Resonance (NMR) is a non-invasive and non-destructive technique that occurs when spinning nuclei in a sample, such as human blood nuclei, are placed in an NMR spectrometer magnetic field (Rasheed *et al*., 2024; Rasheed and Usman, 2023). When the nuclei are subjected to a radio frequency (RF) pulse, the nuclei absorb energy from the RF field and become aligned with the magnetic field. Since this alignment is unstable, the nuclei eventually go back to their previous arrangement, emitting RF radiation in the process (Rahman and Choudhary, 2015). NMR can be utilized to determine the chemical and physical properties of atoms of a sample such as human blood

*Corresponding author. Tel.: +2347065698273
E-mail address: lateefrasheed01@gmail.com (Rasheed A. Lateef.)
https://doi.org/10.62054/ijdm/0201.14

flowing through human blood vessel (Khan *et al.*, 2022). It can also be used to determine blood flow rate and other medical NMR blood flow parameters such as spin-lattice relaxation time, spin-spin relaxation time, blood flow velocity and blood cross sectional area (De, 2013; Jati *et al*., 2016; Odoh and De, 2008; Rasheed *et al*., 2024; Rasheed and Usman, 2023). NMR is defined by a third order linear partial differential equation called the improved Bloch NMR fluid flow equation. The improved Bloch NMR fluid flow equation is an equation that can be utilized to describe the behavior of blood proton spins flowing through the human blood vessels by modeling the magnetization of the spins as a function of time in the presence of an external magnetic field. The improved Bloch NMR fluid flow equation refers to two types of relaxation: longitudinal relaxation and transverse relaxation. Mathematically, the solution of the improved Bloch NMR time-dependent fluid flow equation can be processed theoretically using the Fourier transformation technique in order to obtain the NMR spectrum. In the context of NMR, the NMR spectrum can be used to determine the number of protons present in a given sample (Awojoyogbe, 2002, 2003; Rasheed *et al.*, 2024; Rasheed and Usman, 2023).

Numerous research studies have been done on NMR spectrum and their applications in medicine, Physics, Pharmacy and Chemistry, as evidenced by the extensive literature and experimental research available (Barker *et al*., 1993; Bathen, 2000; Behar *et al*., 1994; Bryant and Korb, 2005; Castellano and Bothner-By, 1964; Civan and Shporer, 1972; Kawata *et al*., 2004; Marjańska *et al.*, 2012; McNamara *et al.*, 1994; Michaelis *et al*., 1991; Piotto *et al*., 2013; Rabenstein *et al.*, 1988; Ramesh *et al.*, 1986; Roy *et al*., 1990; Smith *et al.*, 2007; Strecker *et al.*, 1989; Tanaka *et al*., 1986; Thompson and Lee, 1986; Tkac *et al.*, 2001). Hofmann *et al*. (2001) conducted a study using short-echo time magnetic resonance (MR) spectroscopy to analyze the human brain. They simultaneously recorded the completely relaxed metabolite spectrum and the macromolecular baseline using a sequence of saturation recovery scans. Forty patients had both white and gray matter treated using this method. The study found that the macromolecular content and composition varied depending on the cerebral location and the age of the subjects, although no differences were observed based on gender. Rothan *et al*. (1973) employed spin-echo homonuclear double-resonance difference approach to segregate alanine, lactate, glutamate, glutamine, and β-hydroxybutyrate resonances from overlapping lipid resonance. They concluded that this method improves the detection of different metabolites by efficiently streamlining the analysis of hydrogen NMR spectrum in biological tissues. Campbell *et al.* (1973) reported that subtracting a widened spectrum from the original spectrum improved the resolution of complex NMR spectra. They used hen egg white lysozymes as their materials. Their study concluded that the methods used significantly increase clarity and detail in examining protein NMR spectra. Mendz *et al.* (1989) carried out a study titled Identification of Methyl Resonances in the 1H NMR Spectrum of Incubated Blood Cell Lysates. They investigated low-frequency methyl resonances using lysates from cultured blood cells. They concluded that erythrocyte peptidases, membrane and granule proteases, and other enzymes play a role in proteolysis. Kilby *et al.* (1990) investigated the phosphodiester peak, a noticeable component of the 31P NMR spectrum of the human brain observed in vivo. They discovered relaxation times of 2 and 10 milliseconds using methods like bio-exponential transverse relaxation, which correlate to tiny cytosolic phosphates such as glycerol phosphorethanolamine and glycerol phosphocholine as well as bilayer lipids. They concluded that this approach greatly advances biochemical analysis in neurological research by precisely quantifying brain metabolites and successfully elucidating the source of phosphodiester components. Pappu *et al.* (1993) used non-linear least-squares approach based on the Levenberg-Marquardt method to calculate the parameters of these resonances. Their findings showed certain half widths and intensity ratios are applicable to both methyl and methylene resonances.

Previous studies have utilized techniques such as the bio-exponential spin-spin relaxation method, non-linear least square method, recovery saturation (SR) method, paramagnetic difference (PD) method, and convolution difference (CD) method to analyze and generate NMR spectrum. Building upon these findings, this research work seeks to theoretically analyze and investigate, using an improved Bloch NMR fluid flow equation and Fourier Transform (FT), the effect of transverse relaxation times of arterial, venous, and capillary blood samples on the area under the spectrum of human spinning blood protons.

1.1 NMR Signal of Blood Spinning Protons

The NMR signal, which is also known as the free induction decay (FID) signal, is the magnetization of blood-spinning protons flowing through human vessels at the transient state, defined by the improved Bloch NMR fluid flow equation given as follows (Rasheed *et al*., 2024).

$$v^3T_1T_2^2\frac{\partial^3M_y}{\partial x^3}+T_1T_2^2\frac{\partial^3M_y}{\partial t^3}+3v^3T_1T_2^2\frac{\partial^3M_y}{\partial t\partial x^2}+3vT_1T_2^2\frac{\partial^3M_y}{\partial x\partial t^2}+\left(2v^2T_1T_2+v^2T_2^2\right)\frac{\partial^2M_y}{\partial x^2}+\left(4vT_1T_2+2vT_2^2\right)\frac{\partial^2M_y}{\partial x\partial t}$$
$$+\left(T_2^2+2T_1T_2\right)\frac{\partial^2M_y}{\partial t^2}+\left(T_1+2T_2\right)\frac{\partial M_y}{\partial t}+\left(2vT_2+vT_1\right)\frac{\partial M_y}{\partial x}+\left(T_1T_2\gamma^2B_1^2+\gamma^2T_2^2B_0^2+1\right)M_y$$
$$=T_2\gamma B_1M_0\left(\cos\omega t-2T_2\gamma B_0\sin\omega t\right) \quad (1)$$

In nuclear magnetic resonance (NMR), transient state refers to the state where the magnetization of a sample, such as human blood, remains unchanged with distance. When blood flows uniformly within a human blood vessel, the transverse magnetization, M_y, becomes spatially uniform, and all the partial derivatives with respect to the variable x in the improved Bloch NMR fluid flow space-time-dependent equation (1) can be set to zero. This reduces the improved Bloch NMR fluid flow space-time-dependent equation (1) to the improved Bloch NMR fluid flow time-dependent equation. Thus, Eq. (1) becomes:

$$\frac{d^3M_y}{dt^3}+\left(\frac{T_2+2T_1}{T_1T_2}\right)\frac{d^2M_y}{dt^2}+\left(\frac{T_1+2T_2}{T_1T_2^2}\right)\frac{dM_y}{dt}+\left(\frac{T_1T_2\gamma^2B_1^2+T_2^2\gamma^2B_0^2+1}{T_1T_2^2}\right)M_y$$
$$=\frac{\gamma B_1M_0}{v^3T_1\left(\dfrac{\cos\omega t}{T_2}-2\gamma B_0\sin\omega t\right)} \quad (2)$$

where M_y is the NMR signal of the spinning protons, T_1 is the longitudinal relaxation time of blood spinning protons, T_2 is transverse relaxation time of blood spinning protons, γ is the gyromagnetic of blood spinning protons, B_0 is the static magnetic field, B_1 is the radio-frequency (RF) magnetic field and ω is the Larmor frequency of the blood spinning protons.

Eq. (2) in this research work is the improved Bloch NMR fluid flow time-dependent equation, which models the temporal evolution of the magnetization of human blood spinning protons in an NMR experiment. Eq. (2) has been analytically solved using the Laplace transform method. This yields an exact solution which represents NMR signal of the spinning protons, given as follows:

$$M_y(t)=2\left(a_{21}\cos\omega t+a_{22}\sin\omega t\right)+2e^{a_{15}t}\left(a_{27}\cos a_{16}t+a_{28}\sin a_{16}t\right)+a_{29}e^{s_3t} \quad (3)$$

Eq. (3) incorporates the symbols s_3 and a_i (i = 6, …, 26), which have the following definitions:

$$a_6=ka_1 \quad (4)$$
$$a_7=ka_2+\omega^2k \quad (5)$$
$$a_8=\omega^2a_1k+a_4 \quad (6)$$
$$a_9=\omega^2ka_2+a_5\omega \quad (7)$$
$$a_{10}=3a_2+3\omega^2 \quad (8)$$
$$a_{11}=2a_3+2a_1\omega^2 \quad (9)$$
$$a_{12}=\omega^2a_2 \quad (10)$$
$$a_{13}=\frac{3a_2-a_1^2}{3} \quad (11)$$
$$a_{14}=\frac{2a_1^3+27a_3-9a_1a_2}{27} \quad (12)$$

$$G = \frac{a_{14}}{2} \tag{13}$$

$$H = \sqrt{\frac{a_{13}}{27} + \frac{a_{14}}{4}} \tag{14}$$

$$s_3 = \left(-G + H\right)^{\frac{1}{3}} + \left(-G - H\right)^{\frac{1}{3}} - a_1/3 \tag{15}$$

$$a_{15} = -\left(\frac{a_1 + s_3}{2}\right) \tag{16}$$

$$a_{16} = \frac{\sqrt{3s_3^2 + 2a_1 s_3 + 4a_2 - a_1^2}}{2} \tag{17}$$

$$a_{17} = k\omega^4 + a_9 - a_7\omega^2 \tag{18}$$

$$a_{18} = a_6\omega^3 - a_8\omega \tag{19}$$

$$a_{19} = 5\omega^4 + a_{12} - a_{10}\omega^2 \tag{20}$$

$$a_{20} = 4a_1\omega^3 - a_{11}\omega \tag{21}$$

$$a_{21} = \frac{a_{17}a_{19} + a_{18}a_{20}}{a_{19}^2 + a_{20}^2} \tag{22}$$

$$a_{22} = \frac{a_{18}a_{19} - a_{17}a_{20}}{a_{19}^2 + a_{20}^2} \tag{23}$$

$$\begin{aligned} a_{23} = {} & k\left(a_{15}^4 + a_{16}^4 - 6a_{15}^2a_{16}^2\right) + a_6\left(a_{15}^3 - 3a_{15}a_{16}^2\right) \\ & + a_7\left(a_{15}^2 - a_{16}^2\right) + a_8a_{15} + a_9 \end{aligned} \tag{24}$$

$$a_{24} = 4ka_{15}a_{16}\left(a_{16}^2 - a_{15}^2\right) + a_6a_{16}\left(a_{16}^2 - 3a_{15}^2\right) - a_{16}\left(2a_7a_{15} - a_8\right) \tag{25}$$

$$\begin{aligned} a_{25} = {} & 5\left(a_{15}^4 + a_{16}^4 - 6a_{15}^2a_{16}^2\right) + 4a_1\left(a_{15}^3 - 3a_{15}a_{16}^2\right) \\ & + a_{10}\left(a_{15}^2 - a_{16}^2\right) + a_{11}a_{15} + a_{12} \end{aligned} \tag{26}$$

$$a_{26} = 20a_{16}\left(a_{15}a_{15}^2 - a_{13}^3\right) + 4a_1a_{16}\left(a_{16}^2 - 3a_{15}^2\right) - a_{16}\left(2a_{10}a_{15} - a_{11}\right) \tag{27}$$

1.2 Generation of NMR Spectrum of Blood Spinning Protons using Fourier Transform Signal Processing Technique

In nuclear magnetic resonance (NMR), the Fourier transform signal processing technique is employed to convert the NMR signal from the time domain to the frequency domain, resulting in the generation of the NMR spectrum. In this research work, we used the Fourier transform signal processing technique to take the Fourier transformation of the NMR time-domain signal defined by Eq. (3). Thus, we have a newly developed NMR spectrum equation given as follows:

$$M_y\left(\omega_s\right) = \left[\frac{d_{23}\omega_s^2 + d_{24}\omega_s}{d_2\omega_s^4 + d_3\omega_s^2 + d_1^2}\right]\sin c\left(\omega_s\right) + \left[\frac{d_9\omega_s^2 - d_{10}\omega_s}{d_{11}\omega_s^2 - d_{12}}\right]\sin c\left(T_p\omega_s\right) + \left[\frac{d_{15}\omega_s}{d_{11}\omega_s^2 + d_{16}}\right]\sin c\left(\omega_s\right)$$

$$+\left[\frac{d_{28}\omega_s^3}{d_{11}\omega_s^2-d_{12}}\right]\sin c^2\left(\frac{\omega_s}{2}\right)+\left[\frac{d_{29}\omega_s^2}{d_{11}\omega_s^2+d_{16}}\right]\sin c^2\left(\frac{\omega_s}{2}\right)+\left[\frac{d_{30}\omega_s^4-d_{31}\omega_s^3}{d_2\omega_s^4+d_3\omega_s^2+d_1^2}\right]\sin c^2\left(\frac{\omega_s}{2}\right)$$
$$+\frac{d_{17}\omega_s+d_{35}}{d_{11}\omega_s^2+d_{16}}+\frac{d_{36}\omega_s^3+d_{37}\omega_s}{d_2\omega_s^4+d_3\omega_s^2+d_1^2}+\frac{d_{38}\omega_s}{d_{11}\omega_s^2-d_{12}} \quad (28)$$

where $\sin c(\omega_s), \sin c(T_p\omega_s)$ and $\sin c^2\left(\frac{\omega_s}{2}\right)$ are referred to as sinc functions.

In Eq. (28) the symbols d_i (i = 1, 2, 3,…,38) have the following definitions:

$$d_1 = a_{15}^2T_p^2 + a_{16}^2T_p^2 \quad (29)$$
$$d_2 = \pi^4 \quad (30)$$
$$d_3 = 2\pi^2 d_1 - \left(2\pi a_{16}T_p\right)^2 \quad (31)$$
$$d_4 = \pi d_1 - 2\pi a_{16}^2T_p^2 \quad (32)$$
$$d_5 = 2\pi a_{15}T_p^2\left(a_{27}\cos a_{16}T_p + a_{28}\sin a_{16}T_p\right)e^{a_{15}T_p} \quad (33)$$
$$d_6 = 4a_{15}a_{16}T_p^3\pi^2\left(a_{28}\cos a_{16}T_p - a_{27}\sin a_{16}T_p\right)e^{a_{15}T_p} \quad (34)$$
$$d_7 = 4\pi^2a_{16}^2T_p^3\left(a_{27}\cos a_{16}T_p + a_{28}\sin a_{16}T_p\right)e^{a_{15}T_p} \quad (35)$$
$$d_8 = 2\pi a_{16}T_p^2\left(a_{27}\cos a_{16}T_p - a_{27}\sin a_{16}T_p\right)e^{a_{15}T_p} \quad (36)$$
$$d_9 = 2a_{22}\pi^2T_p^2\cos\omega T_p^2 \quad (37)$$
$$d_{10} = 2a_{21}\pi\omega T_p^3\sin\omega T_p^2 \quad (38)$$
$$d_{11} = \pi^2 \quad (39)$$
$$d_{12} = \left(\omega T_p\right)^2 \quad (40)$$
$$d_{13} = 2a_{27}T_p\pi^3 \quad (41)$$
$$d_{14} = 2a_{27}T_pd_4 \quad (42)$$
$$d_{15} = a_{29}\pi s_3T_p^2e^{s_3T_p} \quad (43)$$
$$d_{16} = \left(T_ps_3\right)^2 \quad (44)$$
$$d_{17} = a_{29}\pi T_p \quad (45)$$
$$d_{18} = 2a_{21}\pi T_p \quad (46)$$
$$d_{19} = 4a_{28}a_{16}a_{15}\pi T_p^3 \quad (47)$$
$$d_{20} = 2\pi^2T_p\left(a_{27}\cos a_{16}T_p + a_{28}\sin a_{16}T_p\right)e^{a_{15}T_p} \quad (48)$$
$$d_{21} = 2\pi^2T_p^2\left(a_{21}\cos\omega T_p^2 + a_{22}\sin\omega T_p^2\right)e^{a_{15}T_p} \quad (49)$$
$$d_{22} = a_{29}\pi^2T_pe^{s_3T_p} \quad (50)$$
$$d_{23} = \pi^2\left(d_5 + d_8\right) \quad (51)$$

$$d_{24} = d_1\left(d_5 - d_8\right) \tag{52}$$

$$d_{25} = d_6 + d_7 - d_{20}d_1 \tag{53}$$

$$d_{26} = d_{20}\pi^2 \tag{54}$$

$$d_{27} = d_{14} - d_{19} \tag{55}$$

$$d_{28} = \frac{\pi d_{21} T_p^3}{2} \tag{56}$$

$$d_{29} = \frac{\pi d_{22}}{2} \tag{57}$$

$$d_{30} = \frac{\pi d_{26}}{2} \tag{58}$$

$$d_{31} = -\frac{\pi d_{25}}{2} \tag{59}$$

$$d_{32} = -\frac{d_{26}}{2} \tag{60}$$

$$d_{33} = \frac{d_{25}}{\pi} \tag{61}$$

$$d_{34} = -\frac{d_{21}}{\pi T_p} \tag{62}$$

$$d_{35} = -\frac{d_{22}}{\pi} \tag{63}$$

$$d_{36} = d_{13} + d_{32} \tag{64}$$

$$d_{37} = d_{27} + d_{33} \tag{65}$$

$$d_{38} = d_{34} + d_{18} \tag{66}$$

2. Materials and Methods

2.1 Materials

2.2 Methods

This study used the Laplace transform method to derive the governing equation for the NMR signal of blood spinning protons, given by Eq. (3), by solving Eq. (2). Additionally, the Fourier transform technique was employed to convert the NMR signal, defined as a function of time in Eq. (3) into the NMR spectrum, which is a function of frequency defined by Eq. (28).

2.3 NMR Blood Flow Constants and Parameters used for Simulations

Eq. (28) defines the NMR spectrum of blood spinning protons, which is a function of NMR blood flow parameters and constants. Thus, we used the values of the NMR blood flow constants and parameters listed in Tables 1 and 2, to investigate the effect of transverse relaxation times of arterial, venous, and capillary blood samples on the area under spectrum of blood proton spins.

Table 1: NMR Blood Flow Constants used for Simulations

NMR Blood Flow Constant	Value	Unit	Source
Gyromagnetic ratio (γ)	2.6752×10^{8}	$rads^{-1}T^{-1}$	(Rasheed *et al.*, 2024)
Equilibrium magnetization (M_0)	1	*A/m*	(Rasheed *et al.*, 2024)
Blood flow velocity (v)	0.2	*m/s*	(Rasheed *et al.*, 2024)
Static magnetic field (B_0)	1.5	*T*	(Rasheed and Usman, 2023)
Radio frequency magnetic field (B_1)	1	*G*	(Rasheed and Usman, 2023)
Longitudinal relaxation time (T_1) for arterial blood sample	1387	*ms*	(Rasheed *et al.*, 2024)
Longitudinal relaxation time (T_1) for venous blood sample	1381	*ms*	(Rasheed *et al.*, 2024)
Longitudinal relaxation time (T_1) for capillary blood sample	300	*ms*	(Rasheed *et al.*, 2024)
Human blood vessel right hand side boundary condition [M(0)]	1	*A/m*	(Rasheed and Usman, 2023)
Human blood vessel left hand side boundary condition [M(L)]	0	*A/m*	(Rasheed and Usman, 2023)
Blood flow pulse duration (T_p)	0.02	*s*	proposed
Length of human blood vessel (L)	0.2	*m*	(Rasheed *et al.*, 2024)

Table 2: NMR Blood Flow Parameters used for Simulations

NMR Blood Flow Parameter	Value	Unit	Source
Transverse relaxation time (T_2) of arterial blood sample	228-280	*ms*	(Rasheed e*t al.*, 2024)
Transverse relaxation time (T_2) of venous blood sample	158-204	*ms*	(Rasheed *et al.*, 2024)
Transverse relaxation time (T_2) of capillary blood sample	10-200	*ms*	(Rasheed *et al.*, 2024)

3. Results and Discussion

3.1 Results

3.1.1 Results of Effect of Transverse Relaxation Time on NMR Spectrum of Signal Generated from Arterial Blood Spinning Protons

Figure 1 with sub-plots (a-d) shows the results of the effect of the blood flow parameter, transverse relaxation time of arterial blood on the NMR spectrum defined by Eq. (28) of the signal generated from arterial blood spinning protons. The results showed that the area under the spectrum of arterial blood spinning protons varied with changes in the arterial blood flow parameters T_2 values of 228 *ms*, 245 *ms*, 262 *ms,* and 279 *ms,* with T_1 set at 1387 *ms.*

3.1.2 Results of Effect of Transverse Relaxation Time on NMR Spectrum of Signal Generated from Venous Blood Spinning Protons

Figure 2 with sub-plots (e-h) depicts the results of the effect of the blood flow parameters, transverse relaxation time of venous blood on the NMR spectrum defined by Eq. (28) of the signal generated from venous blood spinning protons. The results indicated that the area under the spectrum of venous blood spinning protons varied as a function of changes in the venous blood flow parameters T_2 values of 158 *ms*, 173 *ms,* 188 *ms*, and 203 *ms,* with T_1 set at 1381 *ms*.

3.1.3 Results of Effect of Transverse Relaxation Time on NMR Spectrum of Signal Generated from Capillary Blood Spinning Protons

The results of the effect of the blood flow parameters, transverse relaxation time of capillary blood on the NMR spectrum defined by Eq. (28) of the signal generated from capillary blood spinning protons are shown in Figure 3 with sub-plots (i-l). The results revealed that the area under the spectrum of capillary blood spinning protons varied in accordance with changes in capillary blood flow parameters T_2 values of 10 *ms*, 73 *ms*, 136 *ms*, and 199 *ms,* with T_1

set at 300*ms*.

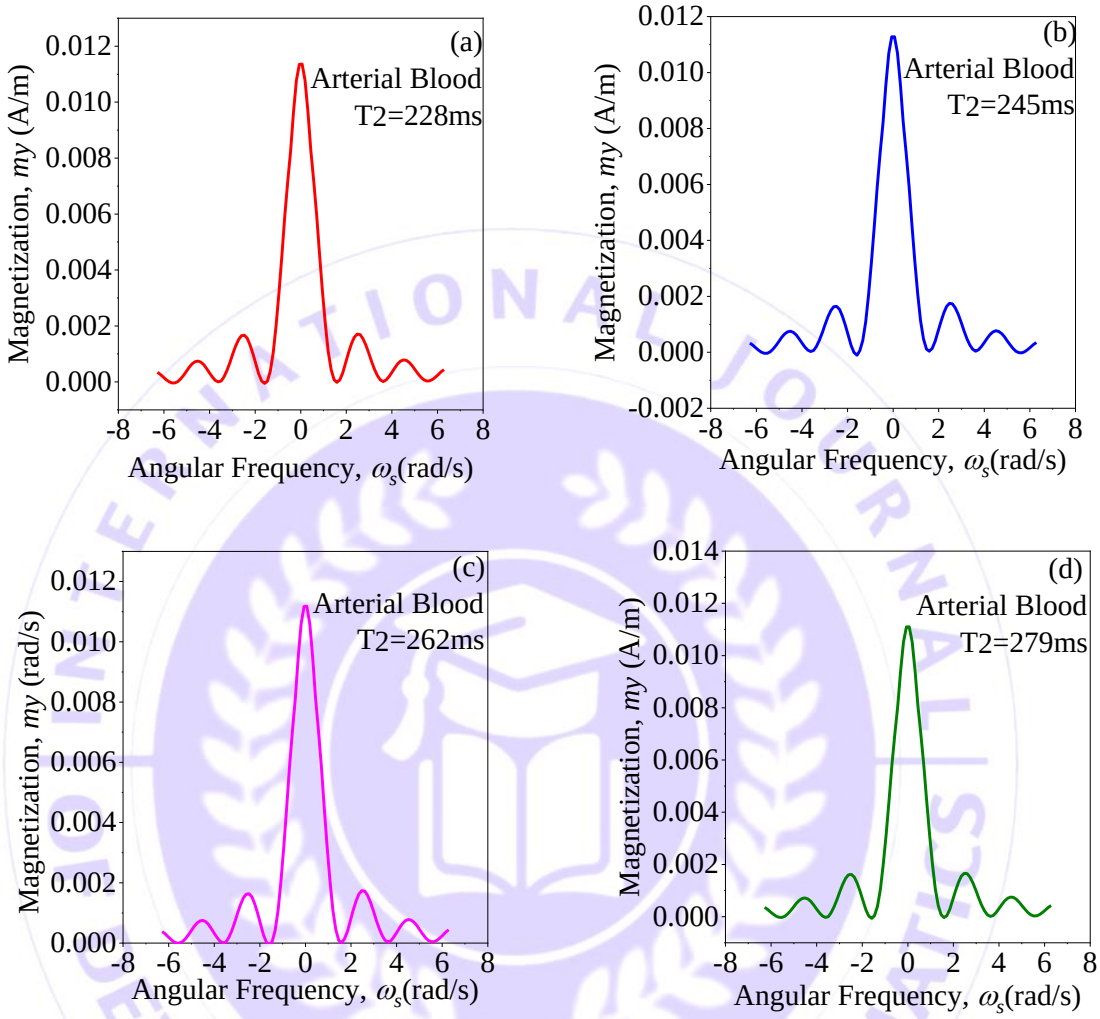

Figure 1: Plots of NMR spectrum defined by Eq. (28) of the NMR signal generated from arterial blood proton spins with (a) T_2 =228ms (b) T_2 =245ms (c) T_2 =262ms (d) T_2 =279ms.

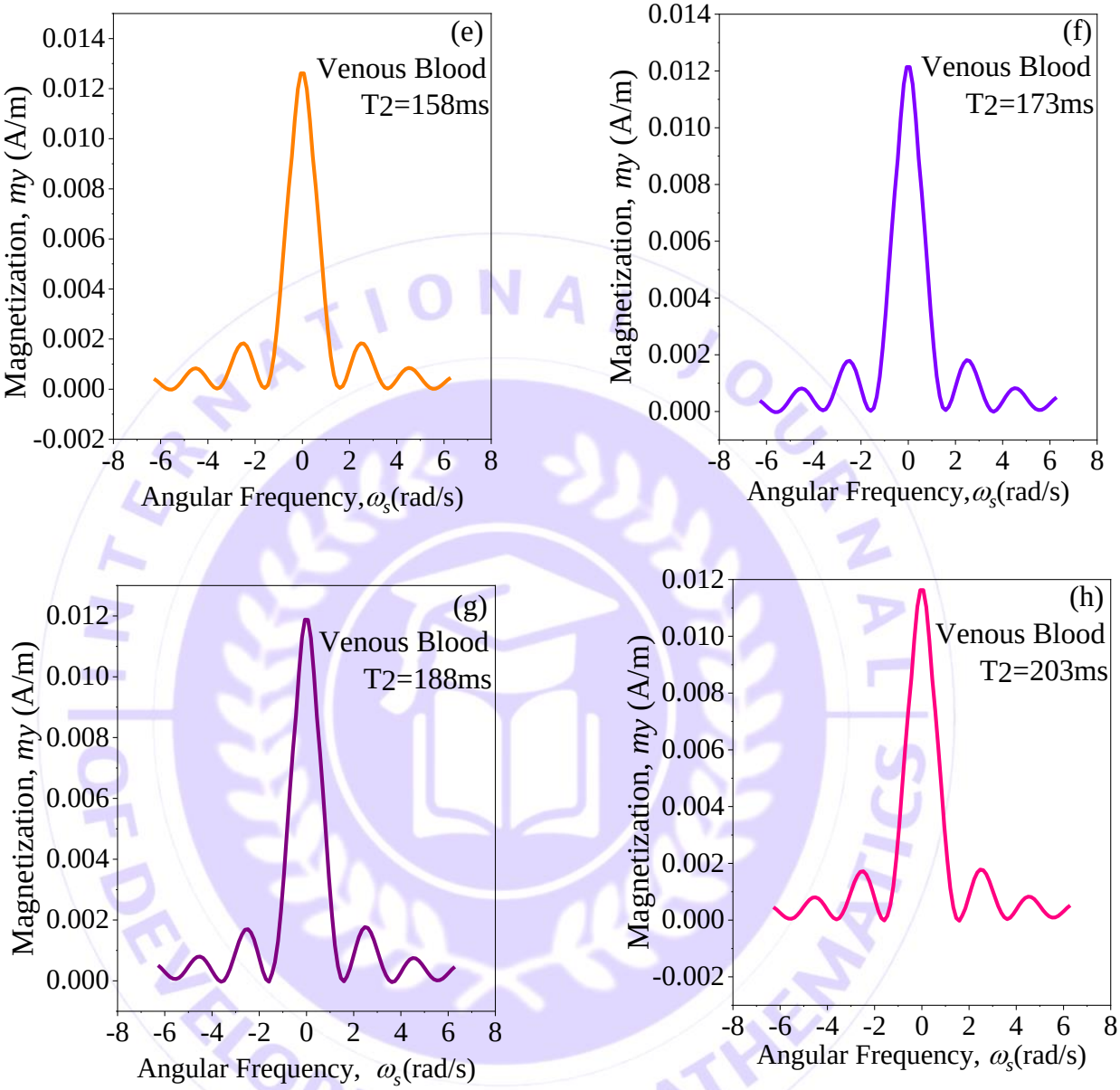

Figure 2: Plots of NMR spectrum defined by Eq. (28) of the NMR signal generated from venous blood proton spins with (e) T_2=158ms (f) T_2 =173ms (g) T_2 =188ms (h) T_2 =203ms.

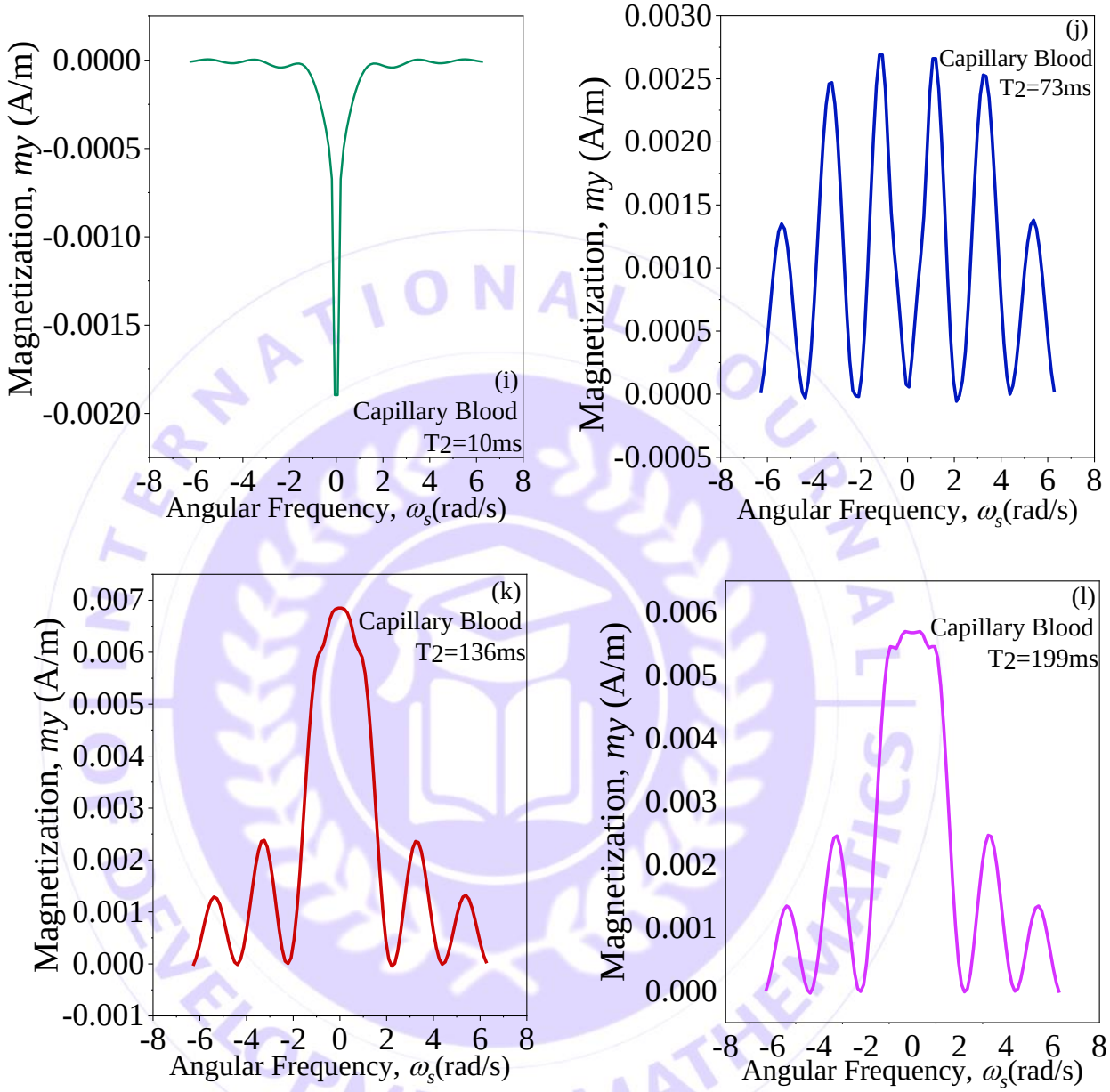

Figure 3: Plots of NMR spectrum defined by Eq. (28) of the NMR signal generated from capillary blood proton spins with (i) T_2 =10ms (j) T_2 =73ms (k) T_2 =136ms (l) T_2 =199ms.

3.2 Discussion

The results for arterial blood samples indicated that the area under the spectrum of arterial blood spinning protons flowing along the human blood vessels, represented by A_s, varied as a function of the arterial blood flow parameter T_2, which changed from 228 *ms* to 279 *ms*. Specifically, the computed values of A_s = 0.02155 $Aradm^{-1}s^{-1}$, 0.02150 $Aradm^{-1}s^{-1}$, 0.02141 $Aradm^{-1}s^{-1}$, and 0.02097 $Aradm^{-1}s^{-1}$ respectively when T_2 = 228 *ms*, 245 *ms*, 262 *ms*, and 279 *ms* at T_1 = 1387 *ms*. This means that changes in the relaxation time of arterial blood proton spins can affect the number of blood-spinning protons in the arterial blood.

The results for venous blood showed that, when venous blood flow parameter T_2 = 158 *ms*, 173 *ms*, 188 *ms*, and 203 *ms* respectively at T_1 = 1381 *ms*, the area under the spectrum of venous blood flowing through the human vessel

has been computed to be As = 0.02416 $Aradm^{-1}s^{-1}$, 0.02334 $Aradm^{-1}s^{-1}$, 0.02270 $Aradm^{-1}s^{-1}$, and 0.02259 $Aradm^{-1}s^{-1}$, respectively. This implies that the number of blood spinning protons in the venous blood is affected by the transverse relaxation time of venous blood proton spins. The results for capillary blood samples revealed that the area under the spectrum of capillary blood spinning protons flowing along the human blood vessel denoted by A_s, varied as a function of changes in the capillary blood flow parameter T_2. The observed simulated values of A_s were found to be 0.00127 $Aradm^{-1}s^{-1}$, 0.01365 $Aradm^{-1}s^{-1}$, 0.02697 $Aradm^{-1}s^{-1}$, and 0.02530 $Aradm^{-1}s^{-1}$, respectively, at T_1 = 300 when T_2 has been set to 10, 73, 136, and 199. This means that the number of spinning protons in the capillary blood is affected by the transverse relaxation time of capillary blood proton spins.

4. Conclusion

In conclusion, this study investigated the effect of the transverse relaxation times of arterial, venous, and capillary blood samples on the area under the NMR spectrum of signal generated from blood proton spins. The study was carried out theoretically by simulating and generating data from the newly developed governing equation for the NMR spectrum, which was derived using Fourier transform signal processing technique. The results for arterial blood samples showed that when the transverse relaxation time of arterial blood sample is 228 *ms*, 245 *ms,* 262 *ms*, and 279 *ms*, respectively, the computed values of area under the spectrum were 0.02155 $Aradm^{-1}s^{-1}$, 0.02150 $Aradm^{-1}s^{-1}$, 0.02141 $Aradm^{-1}s^{-1}$, and 0.02097 $Aradm^{-1}s^{-1}$ respectively. Additionally, the results for the venous blood samples showed that when the transverse relaxation time of venous blood sample is 158 *ms*, 173 *ms*, 188 *ms*, and 203 *ms*, the computed values of the area under the spectrum were 0.02416 $Aradm^{-1}s^{-1}$, 0.02334 $Aradm^{-1}s^{-1}$, 0.02270 $Aradm^{-1}s^{-1}$, and 0.02259 $Aradm^{-1}s^{-1}$, respectively. To conclude, the results for capillary blood showed that when the transverse relaxation time of capillary blood is 10 *ms*, 73 *ms*, 136 *ms*, and 199 *ms*, respectively, the computed values of area under the spectrum were 0.00127$Aradm^{-1}s^{-1}$, 0.01365$Aradm^{-1}s^{-1}$, 0.02697$Aradm^{-1}s^{-1}$, and 0.02530 $Aradm^{-1}s^{-1}$, respectively. These results mean that for varied transverse relaxation times of arterial, venous, and capillary blood samples, the number of blood protons varies over time as blood circulates through the human vessels.

References

Awojoyogbe, O. B. (2002). A mathematical model of the Bloch NMR equations for quantitative analysis of blood flow in blood vessels with changing cross-section-I. *Physica A: Statistical Mechanics and Its Applications*, *303*(1–2), 163–175. https://doi.org/10.1016 /S0378-4371(01)00379-X

Awojoyogbe, O. B. (2003). A mathematical model of Bloch NMR equations for quantitative analysis of blood flow in blood vessels of changing cross-section-Part- II. *Physica A: Statistical Mechanics and Its Applications*, *323*, 534–550. https://doi.org/10.1016/S0378-4371(02)02025-3

Barker, P. B., Soher, B. J., Blackband, S. J., Chatham, J. C., Mathews, V. P., and Bryan, R. N. (1993). Quantitation of proton NMR spectra of the human brain using tissue water as an internal concentration reference. *NMR in Biomedicine*, *6*(1), 89–94. https://doi.org/10.1002/nbm.1940060114

Bathen, T. F. (2000). *NMR Spectroscopy of Blood Plasma: Chemometrics Applied to the Analysis of Proton NMR Spectra of Human Blood Plasma and Its Lipoprotein Fractions*. Norwegian Cancer Society.

Behar, K. L., Rothman, D. L., Spencer, D. D., and Petroff, O. A. C. (1994). Analysis of macromolecule resonances in ^{1}H NMR spectra of human brain. *Magnetic Resonance in Medicine*, *32*(3), 294–302. https://doi.org/10.1002/mrm.1910320304

Bottomley, P. A. (1983). Nuclear magnetic resonance: Beyond physical imaging: A powerful new diagnostic tool that uses magnetic fields and radio waves creates pictures of the body's internal chemistry. *IEEE Spectrum*, *20*(2), 32–38. https://doi.org/ 10.1109/MSPEC.1983.6369002

Bryant, R. G., and Korb, J.-P. (2005). Nuclear magnetic resonance and spin relaxation in biological systems. *Magnetic Resonance Imaging*, *23*(2), 167–173. https://doi.org/10.1016/j.mri.2004.11.026

Campbell, I. D., Dobson, C. M., Williams, R. J. P., and Xavier, A. V. (1973). Resolution enhancement of protein PMR spectra using the difference between a broadened and a normal spectrum. *Journal of Magnetic Resonance (1969)*, *11*(2), 172–181. https://doi.org/10.1016/0022-2364(73)90004-8

Castellano, S., and Bothner-By, A. A. (1964). Analysis of NMR spectra by least squares. *The Journal of Chemical Physics*, *41*(12), 3863–3869. https://doi.org/10.1063/1.1725826

Chittora, N., and Babel, D. (2018). A brief study on Fourier transform and its applications. *Int. Res. J. Eng. Technol.(IRJET)*, *5*(12), 1127–1130.

Civan, M. M., and Shporer, M. (1972). 17O Nuclear magnetic resonance spectrum of H217O in frog striated muscle. *Biophysical Journal*, *12*(4), 404–413.

De, D. K. (2013). NMR/MRI blood flow magnetization equation in the rotating frame of reference-Part I. *Advanced Science, Engineering and Medicine*, *5*(11), Article 11. https://doi.org/10.1166/asem.2013.1404

Dutta, A. (2017). Fourier transform infrared spectroscopy. *Spectroscopic Methods for Nanomaterials Characterization*, 73–93. https://doi.org/10.1016/B978-0-323-46140-5.00004-2

Farrar, T. C. (1978). Pulsed and Fourier Transform NMR Spectroscopy. In *Transform Techniques in Chemistry* (pp. 199–226). Springer.

Hofmann, L., Slotboom, J., Boesch, C., and Kreis, R. (2001). Characterization of the macromolecule baseline in localized[1] H-MR spectra of human brain. *Magnetic Resonance in Medicine*, *46*(5), 855–863. https://doi.org/10.1002/mrm.1269

Hosur, R. V., and Kakita, V. M. R. (2022). Fourier transform NMR. In *A graduate course in NMR spectroscopy* (pp. 89–142). Springer. https://link.springer.com/chapter/10.1007/978-3-030-88769-8_3

Hsu, C.-P. S. (1997). Infrared spectroscopy. *Handbook of Instrumental Techniques for Analytical Chemistry*, *249*.

Hulse, S. G. (2023). *Estimation of NMR signals in the time domain: Methodology, applications and software* [PhD Thesis, University of Oxford].

Jati, B. M. E., SU, A. B. S. B., and Maruto, G. (2016). Blood Pressure Monitoring System Using NMR Method. *EPH-International Journal of Applied Science*, *2*(3), 8–15. https://doi.org/10.53555/eijas.v2i3.17

Katti, G., Ara, S. A., and Shireen, A. (2011). Magnetic resonance imaging (MRI)–A review. *International Journal of Dental Clinics*, *3*(1), 65–70.

Kawata, Y., Kamiya, T., Miura, H., Kimura, A., and Fujiwara, H. (2004). Practical application of NMR spectra of 129Xe dissolved in red blood cell. *International Congress Series*, *1265*, 172–176. https://doi.org/10.1016/j.ics.2004.04.016

Khan, D., Parveen, I., and Sharma, S. (2022). Design, Synthesis and Characterization of Aurone Based α, β-unsaturated Carbonyl-Amino Ligands and their Application in Microwave Assisted Suzuki, Heck and Buchwald Reactions. *Asian Journal of Organic Chemistry*, *11*(1). **https://doi.org/10.1002/ajoc.202100638**

Kilby, P. M., Allis, J. L., and Radda, G. K. (1990). Spin-spin relaxation of the phosphodiester resonance in the[31] P NMR spectrum of human brain: The determination of the concentrations of phosphodiester components. *FEBS Letters*, *272*(1–2), 163–165. https://doi.org/10.1016/0014-5793(90)80474-W.

Marjanska, M., Auerbach, E. J., Valabregue, R., Van De Moortele, P., Adriany, G., and Garwood, M. (2012). Localized[1] H NMR spectroscopy in different regions of human brain *in vivo* at 7 T: T_2 relaxation times and concentrations of cerebral metabolites. *NMR in Biomedicine*, *25*(2), 332–339. https://doi.org/10.1002/nbm.1754.

McNamara, R., Arias-Mendoza, F., and Brown, T. R. (1994). Investigation of broad resonances in[31] P NMR spectra of the human brain *in vivo*. *NMR in Biomedicine*, *7*(5), 237–242. https://doi.org/10.1002/nbm.1940070507.

Mendz, G. L., McCall, M. N., and Kuchel, P. W. (1989). Identification of methyl resonances in the 1H NMR spectrum of incubated blood cell lysates. *Journal of Biological Chemistry*, *264*(4), 2100–2107. https://doi.org/10.1016/S0021-9258(18)94147-5

Michaelis, T., Merboldt, K., Hanicke, W., Gyngell, M. L., Bruhn, H., and Frahm, J. (1991). On the identification of cerebral metabolites in localized[1] H NMR spectra of human brain *In vivo*. *NMR in Biomedicine*, *4*(2), 90–98. https://doi.org/10.1002/nbm.1940040211

Odoh, E. O., and De, D. K. (2008). Application of Nuclear Magnetic Resonance Imaging in Blood Flow Estimation. *The African Review of Physics*, *2*(1).

Pappu, R., Johnson, T. W., Asplund, R. O., and Pierre, J. W. (1993). Spectral estimation of human blood for use in cancer detection. *Proceedings of 36th Midwest Symposium on Circuits and Systems*, 434–437. https://doi.org/10.1109/MWSCAS.1993.342995

Piotto, M., Moussallieh, F.-M., Imperiale, A., Benahmed, M. A., Detour, J., Bellocq, J.-P., Namer, I. J., and Elbayed, K. (2013). *23 Reproducible Sample Preparation and Spectrum Acquisition Techniques for Metabolic Profiling of Human Tissues by Proton High-Resolution Magic Angle Spinning Nuclear Magnetic Resonance*. https://doi.org/10.1017/CBO9780511996634.027

Rabenstein, D. L., Millis, K. K., and Strauss, E. J. (1988). Proton NMR Spectroscopy of Human Blood Plasma and Red Blood Cell. *Analytical Chemistry*, *60*(24), 1380A-1391A. https://doi.org/10.1021/ac00175a713

Rahman, A., and Choudhary, M. I. (2015). *Solving problems with NMR spectroscopy*. Academic Press.

Ramesh, V., Gyenes, M., Patthy, L., and Llinás, M. (1986). The aromatic[1] H-NMR spectrum of plasminogen kringle 4: A comparative study of human, porcine and bovine homologs. *European Journal of Biochemistry*, *159*(3), 581–595. https://doi.org/10.1111/j.1432-1033.1986.tb09925.x

Rasheed, L., Adam, U., Pascal, T., Emeka, A. L., and Salau, R. (2024). Effect of Relaxation Times on Magnetization of Blood Proton Spins at Steady State using Improved Bloch NMR Fluid Flow Equation. *International Journal of Development Mathematics (IJDM)*, *1*(4), 152–165. https://doi.org/10.62054/ijdm/0104.12

Rasheed, L., and Usman, A. (2023). Analytical solution of Bloch NMR fluid flow space–time-dependent equation using laplace transform and complex inversion integral. *International Journal of Modern Physics B*, 2450052. https://doi.org/10.1142/S0217979224500528

Roy, M., Lee, R. W., Brange, J., and Dunn, M. F. (1990). 1H NMR spectrum of the native human insulin monomer. Evidence for conformational differences between the monomer and aggregated forms. *Journal of Biological Chemistry*, *265*(10), 5448–5452. https://doi.org/10.1016/S0021-9258(19)39381-0

Sifuzzaman, M., Islam, M. R., and Ali, M. Z. (2009). *Application of wavelet transform and its advantages compared to Fourier transform*.

Smith, L. M., Maher, A. D., Cloarec, O., Rantalainen, M., Tang, H., Elliott, P., Stamler, J., Lindon, J. C., Holmes, E., and Nicholson, J. K. (2007). Statistical Correlation and Projection Methods for Improved Information Recovery from Diffusion-Edited NMR Spectra of Biological Samples. *Analytical Chemistry*, *79*(15), 5682–5689. https://doi.org/10.1021/ac0703754

Strecker, G., Wieruszeski, J.-M., Michalski, J.-C., and Montreuil, J. (1989). Complete analysis of the1H- and13C-NMR spectra of four blood-group A active oligosaccharides. *Glycoconjugate Journal*, *6*(3), 271–284. https://doi.org/10.1007/BF01047847

Tanaka, C., Naruse, S., Horikawa, Y., Hirakawa, K., Yoshizaki, K., and Nishikawa, H. (1986). Proton nuclear magnetic resonance spectra of brain tumors. *Magnetic Resonance Imaging*, *4*(6), 503–508. https://doi.org/10.1016/0730-725X(86)90031-7

Tasiu, A. R., and Usman, H. (2024). *Computing Fourier Integral using Matlab*..

Thompson, S. N., and Lee, R. W. K. (1986). *Comparison of starvation and infection by Schistosoma mansoni on tissue viability and the 31 P NMR spectrum of Biomphalaria glabrata.* https://www.cabidigitallibrary.org/doi/full/10.5555/19860837154

Tkac, I., Andersen, P., Adriany, G., Merkle, H., Ugurbil, K., and Gruetter, R. (2001). In vivo^{1} H NMR spectroscopy of the human brain at 7 T. *Magnetic Resonance in Medicine*, *46*(3), 451–456. https://doi.org/10.1002/mrm.1213

Tsybin, Y. O., Nagornov, K. O., and Kozhinov, A. N. (2019). Advanced fundamentals in Fourier transform mass spectrometry. In *Fundamentals and applications of Fourier transform mass spectrometry* (pp. 113–132). https://doi.org/10.1016/B978-0-12-814013-0.00005-3